Transactions, **SMiRT-25**

Charlotte, NC, USA, August 4-9, 2019
Division II – Fracture Mechanics and Structural Integrity

CONSTRAINT EFFECTS WHEN DETERMINING FRATURE TOUGHNESS/MATERIAL FRACTURE RESISTANCE FROM SURFACE-CRAKED ELBOWS, SENT, AND CT SPECIMENS

Suresh Kalyanam, Gery Wilkowski, Yunior Hioe, Frederick Brust, Edward Punch

Engineering Mechanics Corporation of Columbus, Columbus, OH, USA (sureshk@emc-sq.com)

INTRODUCTION

Although the work on the fracture behaviour of elbows has been pursued for several decades, since the 1980s (International Piping Integrity Research Group Phase 2), there is recent interest in a more detailed characterization of the elastic-plastic behaviour of the elbows with surface or through-wall cracks and development of J-estimation schemes. Out of the few pressurized (15.513 MPa, *i.e* 2,250 psi) and elevated temperature (288 C, *i.e* 550 F) elbow experiments conducted in IPIRG-2, the elbow Experiment 2-4 conducted on TP304 stainless steel was selected for evaluation of the role of constraint between the various specimen geometries SENT, CT, and inner diameter surface-cracked (ID SC) elbow. This was envisaged to lead to improvement of methodologies towards the use of more recent SENT and more traditionally used CT specimen fracture toughness values to determine the fracture behaviour of surface-cracked elbows.

While CT specimen tests were conducted at elevated temperature of 288 C (550 F) on solution-annealed TP304 elbow material from the same heat, no SENT tests were conducted on the IPIRG-2 elbow test TP304 material. Until more recently, it was common practice to assume that the CT specimen provided conservative values (lower bound) of the fracture toughness. However, this IPIRG elbow 2-4 tested had an ID surface-crack that was half the circumference and 70% of the wall thickness on the center-plane of the elbow and centered on the extrados of the elbow (tested under in-plane bending loads in the elbow closing direction) and is know from recent work over last 2 decades that it is more closely represented by a SENT specimen. From a technical standpoint, several researchers from oil and gas and nuclear industries have considered the SENT specimen fracture toughness as comparable to surface-cracked pipe and have used it in their engineering critical assessment or other failure assessments. In recently conducted experiments it was found that the toughness of circumferentially surface-cracked pipe was much higher than the corresponding depth (a/W) SENT specimens [Hioe, Kalyanam *et al.*]. Further, the SENT specimens with various crack depth showed a linear variation in fracture toughness (CTOD values that were determined using double clip-gage method) with crack depth (a/W) such that it was smaller for deeper cracks. On the other hand, in recently examined IPIRG-2 elbow TP304 material, the fracture toughness (elastic-plastic J values using an eta factor method for calculations) of the tested CT specimen (a/W=0.5) was much higher than the tested elbow with crack depth of a/t=0.7.

For making a comparison of all three geometries, SENT, CT, and the component (tested elbow with ID SC), one of the tested CT specimens was reconstituted into two SENT specimens using the region of material that did not suffer any deformation. It is common practice to match the normalized crack depth of the SENT specimen to that in the tested component (to replicate the constraint in the two specimens), and hence in this case the SENT specimens were machined to an initial crack depth, a/W=0.68, corresponding to the deepest point in the initial surface crack in the fatigue precracked IPIRG-2 Elbow Experiment 2-4. Although the crack depth from fatigue precracking was variable around the length of the ID surface crack, it was documented in the IPIRG-2 reports and used for this work. The use of the variable thickness, crack depth, and ovalization of the elbow in this investigation is an area of ongoing research at Emc^2 and also others around the world.

It is more recently understood that the effects of ovalization, variable crack depth, and thickness of the elbow around the circumference needs to be modelled accurately, and was hence captured using a more precise FE mesh of the elbow and attached pipes developed using Emc^2 Piping FEA Software [PipeFracCAE©], which is a state-of-the-art Emc^2 elbow FE mesh generator. These developments led to predictions that were more accurate than those obtained from earlier FE analyses conducted with idealized thickness and crack depth in the elbow 2-4, which in turn provided more accurate guidelines for the choice of crack depth (*i.e* a/W=0.68) in the duplicate SENT specimens tested in this investigation.

ABSTRACT

Fracture parameters (J, CTOD, CMOD) were evaluated for a circumferentially surface-cracked Elbow 2-4, tested (in closing bending moment and internal pressure of 15.51 MPa (2,250 psig) at 288 C (550 F)) as part of the International Piping Integrity Research Group (IPIRG-2) program. Although the inner diameter (ID) surface-crack (SC) was centered on the extrados, the ID SC depth was variable with the greatest being at about 45-degrees from the extrados. To determine the role of constraint on the fracture toughness, a state-of-the-art FEA of the tested elbow was conducted, which included the variable ID SC, variable elbow center-plane thickness, and the initial center-plane ovalization in the 3D FEA model. Using the FEA results, the initial flaw depth for the duplicate single-edge notch tension (SENT) specimens was selected to be a_o/W=0.68, corresponding to the largest J-value in the elbow experiment. The C(T) specimen provided much higher J-values at crack initiation, J_i=6.2 ksi-inch (1.086 MN/m), while the elbow was lower at J_i=2.8 ksi-inch (0.490 MN/m), and the SENT was lowest at J_i=2.1 ksi-inch (0.368 Mn/m). The J_i value of the C(T) specimen was close to 2.5 times that of the elbow, and close to 3 times that of the SENT specimen. J_i and crack-tip opening displacement at crack-initiation ($CTOD_i$) values comparisons indicated that there was a slight difference in the constraint between a comparable normalized depth SENT specimen in the L-R orientation and elbow specimen with ID SC. Until recently, C(T) specimen toughness had been assumed to be a lower-bound estimate, while the results from this investigation suggest otherwise, and a closer constraint representation was found between the SENT and elbow specimen with ID SC for these deep flaws. A second interesting finding from state-of-the-art 3D FEA of the elbow experiment was that the maximum J-value occurred at positions that were 45-degree away from the extrados position on the center-plane of the long-radius 90-degree elbow. For both fracture and stress corrosion cracking (SCC) of elbows, this study suggests that caution should be exercised when selecting the crack locations for structural integrity evaluations of surface-cracked elbows, and it could be more critical to consider a crack centered closer to the 45-degrees from the extrados.

IPIRG-2 CRACKED ELBOW EXPERIMENT 2-4 – FE MODELING AND ANALYSIS

PipeFracCAE© was developed to generate FEA mesh of elbows (used in ABAQUS) with the variability in thickness, initial ovalization of the elbow cross-section, and the surface crack depth

variability around the crack length with several points specified with a/t variation (40 points is commonly used in PipeFracCAE©. The characterization of the thickness from the IPIRG-2 investigation of Elbow 2-4 [Fleming *et al.*] is shown in Table 1 that varies from 0.522 to 0.702 [Fleming *et al.*]) which had a set of 41 points. The thickness variation over the entire central-plane cross-section of the Elbow 2-4 is shown in Figure 1 along with the view of the FEA mesh cross-section in the surface-cracked center-plane of the elbow. Since there was both thickness variation and the ovalization variation (-0.10 inch from intrados to extrados, and +0.10 inch from side-to-side (flank to flank) that were observed, they were modelled in the center-plane of the elbow and both variations (ovalization, and thickness) made to linearly decay to zero at the ends of the 90-degree long-radius elbow as they join the horizontal and vertical pipes used in the elbow experiment. The FEA model comprised of 8-node reduced integration brick elements (C3D8R) with 196,631 nodes and 177,636 elements.

Table 1: Measurements of thickness and flaw depth in the Elbow Experiment 2-4 [Fleming *et al.*].

Location	Pipe Wall thickness, t inch	Precrack Depth, B inch	Initial a/t		Location	Pipe Wall thickness, t inch	Precrack Depth, B inch	Initial a/t
-20	1.292	0.907	0.702		Centerline	1.175	0.630	0.536
-19	1.276	0.857	0.671		1	1.175	0.623	0.530
-18	1.261	0.898	0.655		2	1.175	0.614	0.522
-17	1.260	0.942	0.681		3	1.180	0.622	0.527
-16	1.260	0.967	0.665		4	1.184	0.602	0.508
-15	1.249	0.912	0.641		5	1.184	0.666	0.562
-14	1.238	0.904	0.659		6	1.188	0.704	0.593
-13	1.218	0.806	0.622		7	1.191	0.721	0.605
-12	1.210	0.829	0.626		8	1.193	0.799	0.628
-11	1.203	0.824	0.635		9	1.196	0.832	0.626
-10	1.197	0.823	0.630		10	1.214	0.875	0.622
-9	1.191	0.819	0.635		11	1.232	0.847	0.600
-8	1.188	0.759	0.611		12	1.232	0.854	0.605
-7	1.184	0.739	0.615		13	1.242	0.849	0.623
-6	1.183	0.721	0.609		14	1.252	0.825	0.623
-5	1.181	0.721	0.610		15	1.262	0.811	0.605
-4	1.178	0.699	0.593		16	1.272	0.825	0.624
-3	1.174	0.726	0.618		17	1.271	0.815	0.626
-2	1.174	0.690	0.588		18	1.270	0.825	0.640
-1	1.175	0.667	0.568		19	1.284	0.836	0.651
Centerline	1.175	0.630	0.536		20	1.298	0.887	0.683

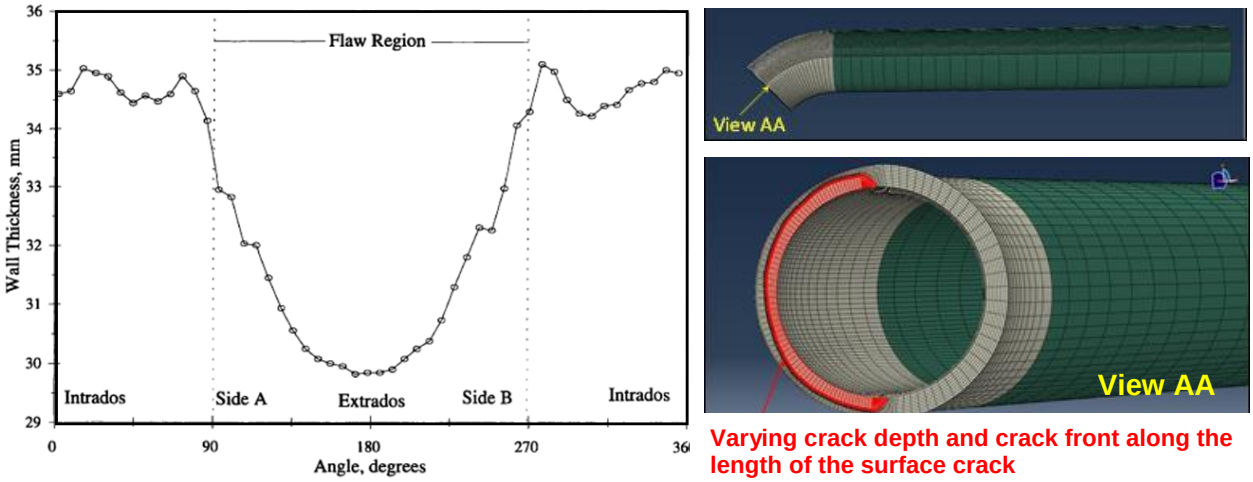

Figure 1. Wall thickness variations in flawed and unflawed regions in the plane going from the extrados to intrados of the 90-degree elbow used in the IPIRG-2 elbow fracture Experiment 2-4 [Fleming *et al.*], and cross-section view of the elbow specimen showing the variation of the surface crack in the extrados along the 180-degree length (half the elbow circumference) and centered on the extrados .

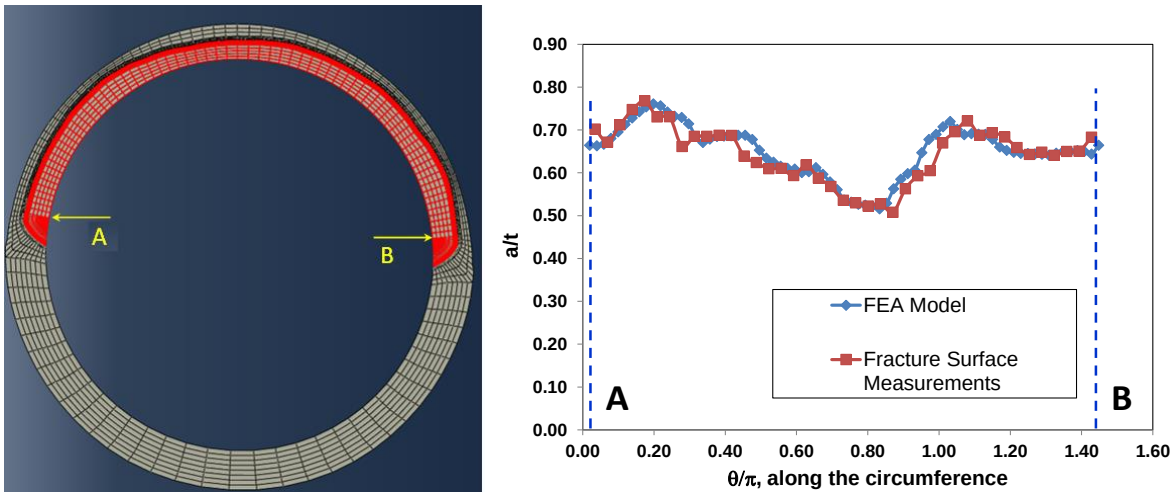

Figure 2. Comparison of the measured variation of the surface-crack depth (after fatigue precracking) with the surface-crack depth in the created mesh for the elbow FE analyses using Emc^2 Piping FE Software [PipeFracCAE©].

Figure 3 presents a sketch of the IPIRG-2 elbow test frame for the elbow bend Experiment 2-4 and the FE model with the boundary conditions and applied displacements (using a wire rope). Hence, in Figure 4 the displacements were applied along the top surface nodes (spanning a circumferential length of 180 degrees) at the end of the horizontal pipe to simulate the experimental wire rope design in the FEA. The three material regions, elbow made of TP304 and the two attached pipes made of A710 Grade-A carbon steel with higher strength are also shown in Figure 4. Apart from the gradual transition of the element lengths from the center ID SC plane to the ends of the elbow, a weld taper was also modelled to account for thickness differences in the elbow and straight pipe.

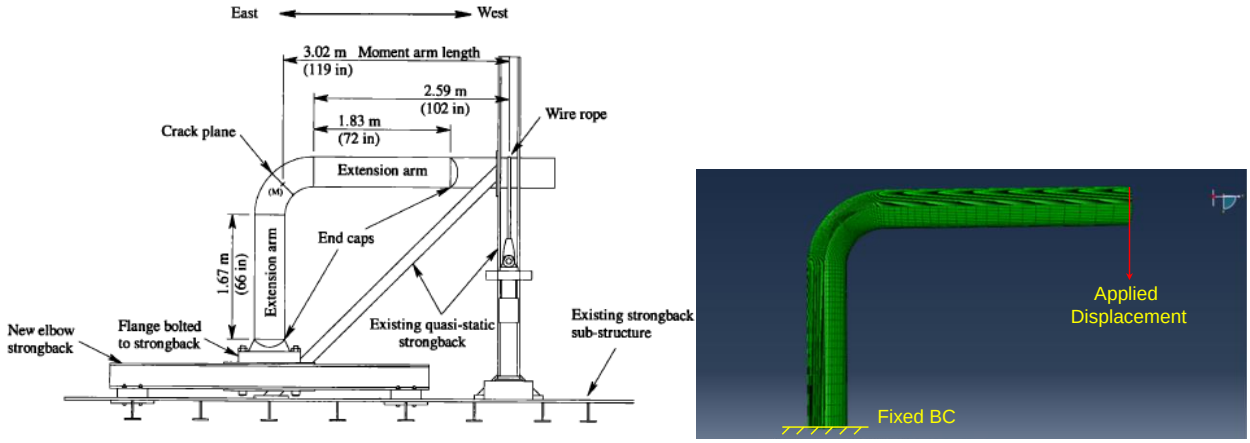

Figure 3. IPIRG-2 elbow Experiment 2-4 set-up [Fleming *et al.*] and model of the elbow test frame used in the FEA with boundary conditions and the wire rope loads applied along the outer surface nodes.

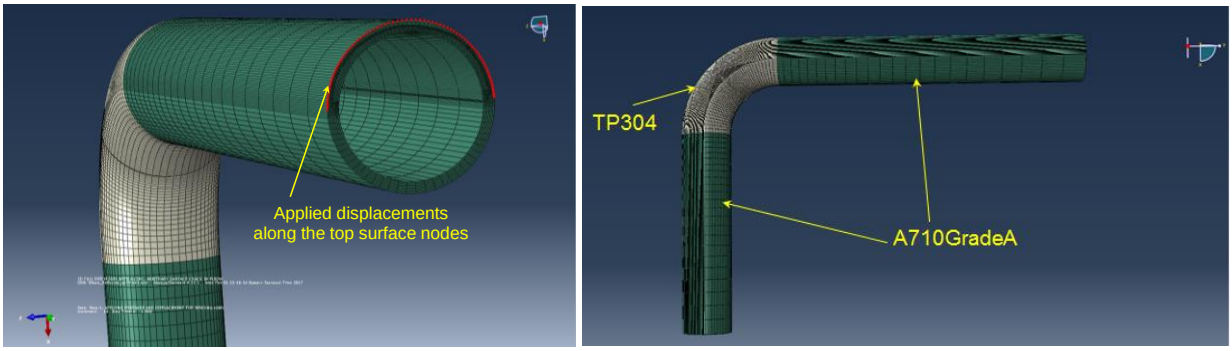

Figure 4. Model of the elbow test frame used in the FE analyses with boundary conditions and the wire rope loads application along the outer surface nodes. Also seen are the three material regions.

To conduct an elastic-plastic analysis a spider mesh with six contours for evaluation of fracture parameter J, and a key-hole mesh with 0.005 inch notch/crack-tip radius (generally used for convergence in elastic-plastic FEA and also providing a crack front stress field solution) was modelled as shown in Figure 5.

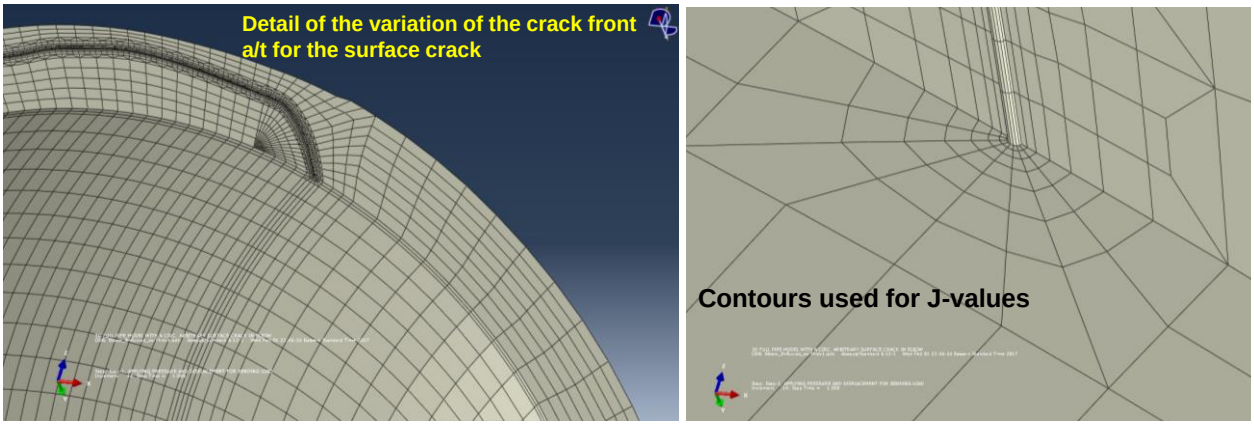

Figure 5. Elbow mesh showing the contours and key-hole geometry at the crack tip used in obtaining the elastic-plastic fracture toughness parameter, J-values from the FEA.

FE Analyses Inputs and Results from the Cracked Elbow FE Modelling to Obtain Appropriate SENT Specimen Flaw Depth

Figure 6 shows the true stress versus logarithmic strain obtained for TP304 material by averaging the duplicate tensile test (AE1-T3, AE1-T4) results from the IPIRG-2 program [Fleming *et al.*]. Owing to the few data points available near the yield stress region, an average trend in the true stress versus logarithmic strain was used to determine FEA inputs, such that a set of 36 points in all were selected to represent the nonlinear material behaviour of the TP304 elbow at 550F (288 C). Since the A710-Grade A carbon steel material has higher strength it was modelled as an elastic material. The material properties of both the materials (TP304, and A710 Grade-A) used in the elbow test FEA is shown in Table 2, and Table 3 provides the experimental parameters (pressure, displacement parameters) corresponding to surface crack initiation and maximum load observed during the IPIRG-2 elbow Experiment 2-4.

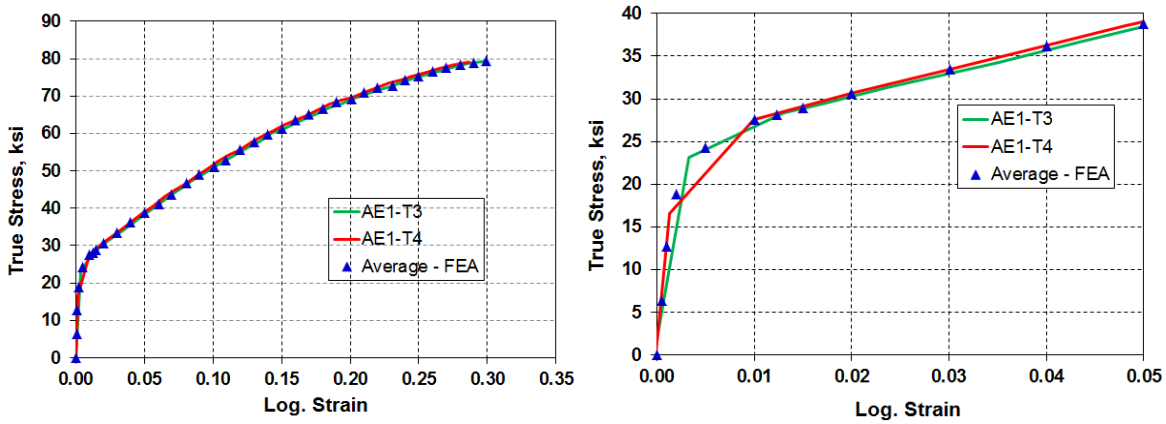

Figure 6. True-stress versus logarithmic strain curve from the two tensile specimens, the discrete set of points selected for the FEA input, and close-up near the yield stress region.

Table 2 provides material properties for the TP304L and the A710 Grade-A materials used in the elbow test FEA. Since the A710 Grade-A straight pipe had a much higher strength than the TP304L elbow material, only the elastic material properties were provided for the carbon-steel straight-pipe material. Table 3 provides the internal pressure used in the experiment and the displacement loads corresponding to the crack initiation and the maximum load observed in the IPIRG-2 elbow Experiment 2-4.

Table 2: Tensile test properties used for the two materials in the elbow test

Specimen Number	Elastic Modulus, ksi	Poisson's ratio	Yield Stress, ksi
TP304	12,745	0.3	18.87
A710 Grade-A	26,650	0.3	–

Note, in several other situations it was seen that TP304 has much lower elastic modulus than design values – in some cases involving confirmatory testing by 3 independent laboratories

Table 3: FE analysis parameters used for the crack initiation and maximum load conditions in the simulation of the IPIRG-2 elbow Experiment 2-4

Simulation Parameter	Value	Units
Internal Pressure	2,250	psi
Displacement – Crack Initiation	6.5	inch
Displacement – Maximum Moment	7.3	inch

Calculated moments from FEA at M_{FEA} = 4,823 inch-kips (545.1 kN-m) were within 1,65% of the moments from the experiment for the crack initiation event, which was $M_{Experiment}$ = 4,745 kip-inch (536.2 kN-m). Table 4 and Table 5 provide the loads and moments from various contributions (elevated temperature and pressurized Elbow experiment 2-4 [Fleming *et al.*]), and those obtained from FEA, respectively for the crack initiation event. The actuator displacement was modelled as wirerope displacement and the internal pressure was applied on the ID surface of the elbow and pipes in the FEA.

Table 4: Elbow Experiment Loads (as in the DRB [Fleming *et al.*])

Total Load	P_{Tot} = Actuator load + P_{ESL}
Dead-weight load	P_{DW} = 1,390 lbs (6.18 kN)
Equivalent Static Load	P_{ESL} = 413 lbs (1.84 kN) $P_{ESL} = P_{DW} - P_{PRESS}$
Static load from pressurization	$P_{PRES} = P_{DW} - P_{ESL}$ = 977 lbs (4.35 kN)

Table 5: Load and Moment Calculations Elbow FEA – Crack Initiation

Load obtained from FEA	P_{FEA} = Actuator load + P_{PRES}= 41,124 lbs (183 kN)
Total load for moment calculation that is akin to the experiment as shown in Table 4	$P_{tot}^{FEA} = P_{FEA} - P_{PRESS} + P_{ESL}$ = 41,124 – 977 + 413 = 40,560 lbs (180.5 kN)
Moment from FEA	$M_{FEA} = P_{Tot}^{FEA}$ × moment arm = 40,560 lbs × 118.9 inch = 4,823 inch-kips = 545 kN-m

Figure 7 shows J-value variations obtained at various load levels (represented as remote load-line displacements applied by the wire rope) along the entire ID SC front. Three of the fracture parameters (J, CMOD, and CTOD) were determined at the crack initiation event of the IPIRG-2 elbow Experiment 2-4 from the FEA. Figure 7 shows the J-values, while Figure 8 shows the CMOD and CTOD values[1] along the ID SC front at the load corresponding to crack initiation. From Figure 7, the maximum J-value was found to occur close to a surface-crack depth of a/t=0.68 near Side-B of the IPIRG-2 elbow Experiment 2-4 and this normalized depth was chosen for the two SENT specimens tested in this investigation.

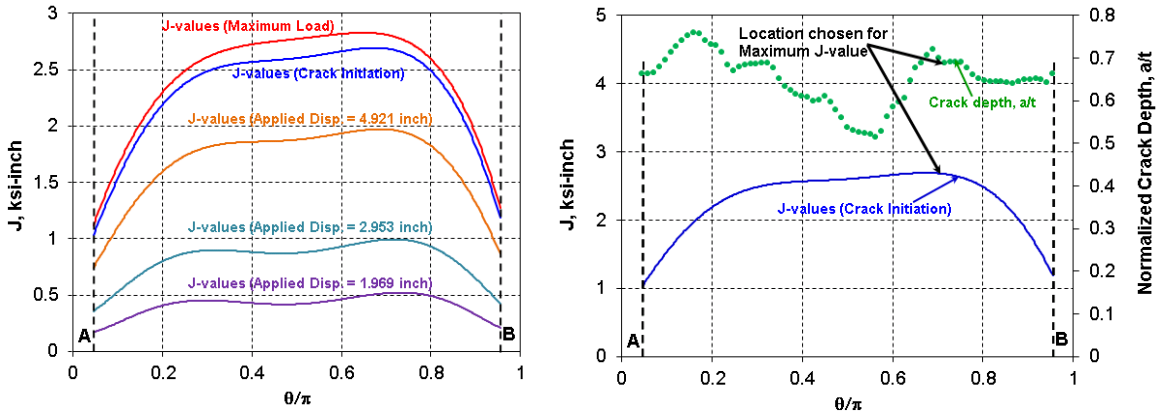

Figure 7. J-values along the surface-crack front of the elbow at different load levels (represented as remote load-line displacements).

[1] CTOD from the elbow FEA was calculated as being equal to the displacements across the diametrically opposite sides of the very small key-hole at the crack tip, which should be close to other FE-based CTOD calculation procedures.

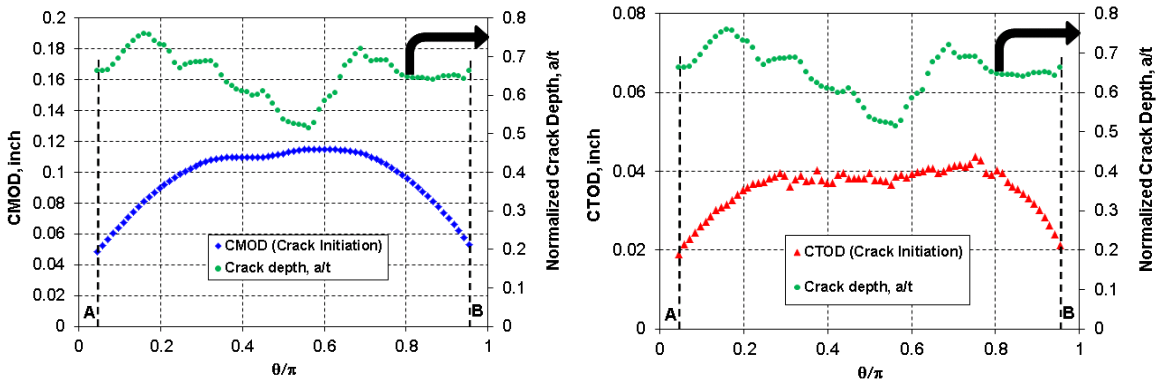

Figure 8. CMOD and CTOD values along the surface-crack front in the IPIRG-2 elbow Experiment 2-4 at the load corresponding to crack initiation.

In spite of the thickness variations in the elbow, maximum J-values along the ID SC front were at about 45-degrees from the center-plane extrados point, which was seen also at lower load levels (Figure 7). Based on these observations from the fatigue precracked Elbow 2-4 (crack was deeper at the 45-degree locations from the extrados), and the elastic-plastic 3D FEA in this investigation there is consistent evidence that the highest crack-driving force may not be centered on the extrados point. This offers the possibility that real circumferential ID SC could be skewed to one/other side of the extrados, and if these cracks were long they might link together in the center at the extrados point (a valuable aspect for designing future tests on elbows).

SENT SPECIMEN PREPARATION TO MATCH ELBOW CRACK DEPTH AND TESTING RESULTS

The broken halves from tested C(T) specimen (shown in Figure 9) were used to make reconstituted SENT specimens (one from each half of the tested C(T) specimen). A careful undertaking included weld build-up for making a double-V weld groove geometry, and welding of extension arms from material similar to the SENT specimens, as shown in Figure 10. It was important to complete the welding with low heat input and further the material was in the solution-annealed condition, sue to which the TP304 stainless steel was not very sensitive to welding temperatures since there is no stress-relief or phase transformation concern. Figure 11 and Figure 12 (close-up view) shows the reconstituted blanks (TP304L welded, machined, and ground) that were used to EDM the SENT specimens E2-4-1 and E2-4-2 (as per illustration in Figure 10). The duplicate SENT specimen were notched to an initial depth of $a_o/W=0.68$ (depth determined from FEA of IPIRG-2 Elbow Experiment 2-4 discussed earlier) using EDM wire (0.004-inch diameter wire to produce a crack that is akin to fatigue precrack) such that the initial crack was in the same orientation as the ID SC in the tested Elbow 2-4 (i.e., L-R orientation). Figure 13 shows the two specimens with the EDM notch machined at the center of the SENT specimen.

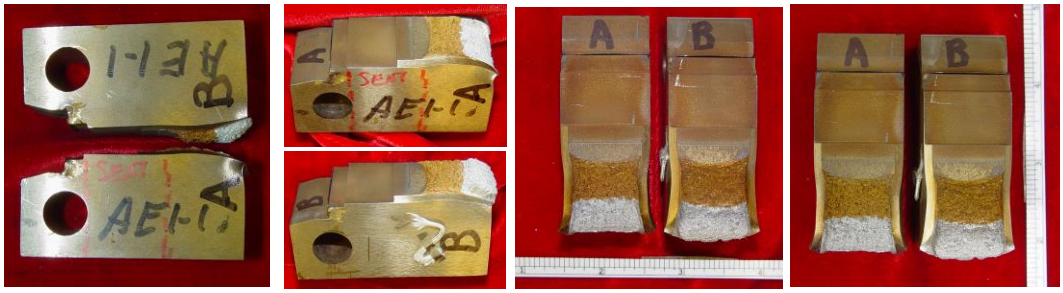

Figure 9. Broken halves of the pedigreed C(T) specimen AE 1-1 from the IPIRG 2-4 elbow test material.

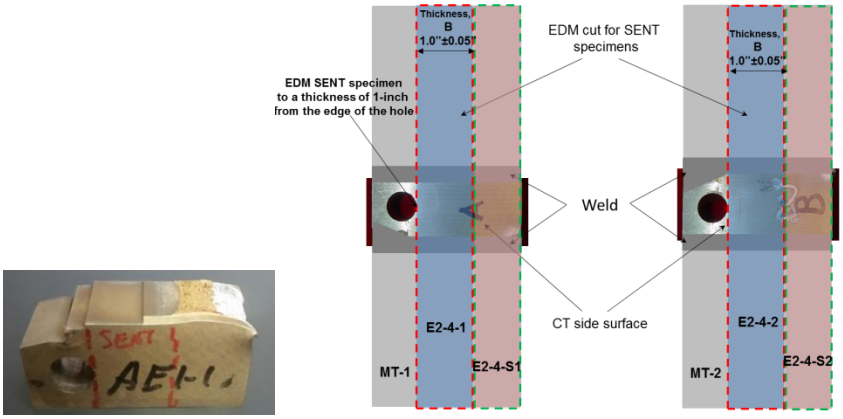

Figure 10. Reconstituted SENT specimen layout from the pedigreed AE 1-1 C(T) specimen originally made from an identical elbow as in the IPIRG-2 elbow Experiment 2-4 (*Note:* E2-4-1 and E2-4-2 are the SENT specimens that were tested in L-R orientation; C(T) specimens were in the L-C orientation).

Figure 11. Reconstituted TP304 blank before machining out the two SENT specimens.

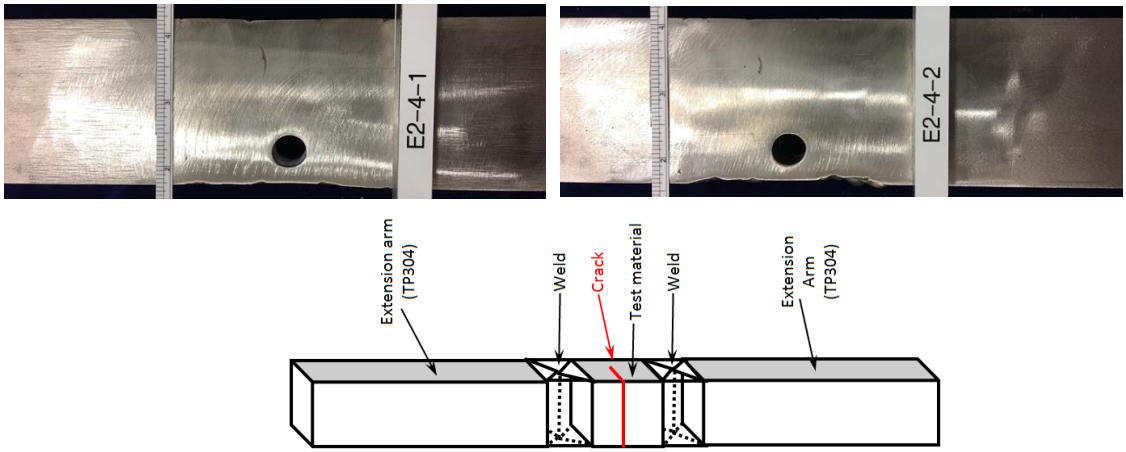

Figure 12. Close-up of reconstituted TP304 blank before machining out the two SENT specimens.

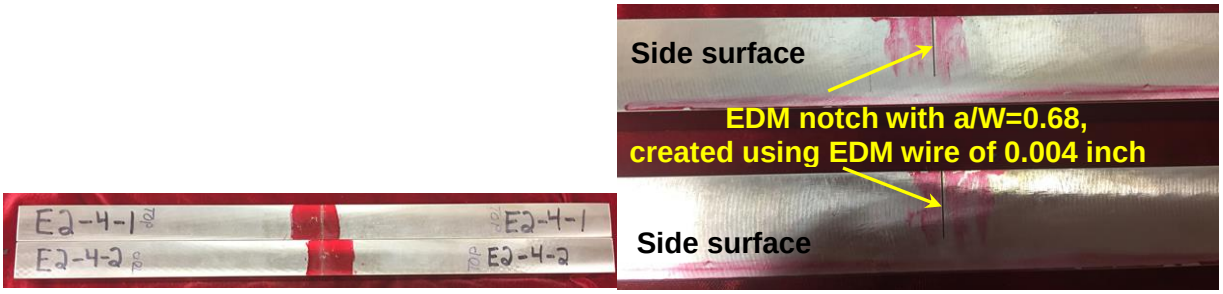

Figure 13. SENT specimens after machining, grinding, and inserting the initial EDM notch.

Blunt-side grooves (notch root radius of 0.063 ± 0.005 inch) were machined to a depth of 5-percent of the thickness (B) on each side of the EDM notch to keep a straight crack front during ductile tearing [Hioe *et al.*]. Double clip-gage stands/blocks (knife edges were at different distances from the specimen surface) were tack welded to the specimens (shown in Figure 14) to obtain the crack-tip-opening displacement (CTOD), a fracture parameter at the initiation of crack growth and the crack-mouth-opening displacement (CMOD) for determining the elastic-plastic fracture toughness parameter, J-value at crack initiation (J_i) and crack-growth resistance curves (J-R and CTOD-R).

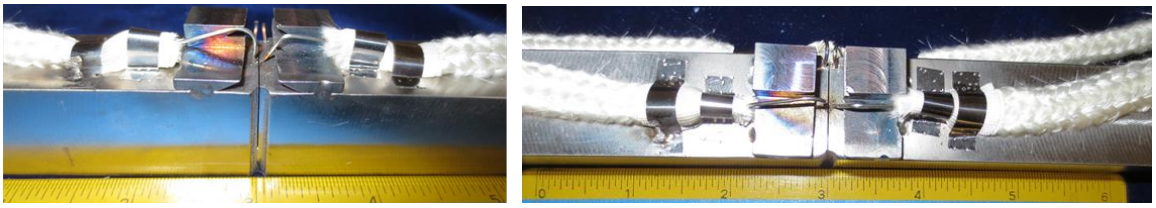

Figure 14. SENT specimen with the dual clip-gage stands and the d-c EP probes for electric-potential measurements across the crack during the test.

SENT tests were conducted in accordance with the DNV recommended practice [DNV-RP-F108], ASTM standard [ASTM E-1820-15a], and Emc^2 experience in SENT testing. To run the SENT test at roughly the same displacement rate, using the time determined for the crack to reach initiation in the IPIRG-2 elbow Experiment 2-4, a corresponding CMOD at crack initiation was computed using FEA of the SENT geometry and using the same material properties as used earlier in the elbow FEA of Experiment 2-4. Using the results from the FEA of the SENT specimen the tests were conducted at 0.0001 inch/sec (an order of magnitude of the time for the elbow to reach the CMOD at crack initiation in 1,958 seconds). Table 6 shows the specimen and pretest and posttest crack dimensions test (measured using ASTM 9-point method as per ASTM standard [ASTM E1820-15a]) for the two SENT specimens.

Table 6: Geometry and Crack dimensions of the two SENT specimens.

Specimen Number	Width (W), inch	Thickness (B), inch	Net-Thickness after side-groove (B_N), inch	Length (L), inch	Initial crack depth (a_o), inch	aa_o/W	Final crack depth (a_p), inch	Crack growth (Δa), inch
E2-4-1	0.921	0.918	0.766	4.96	0.6142	0.667	0.7047	0.0905
E2-4-2	0.921	0.917	0.765	4.96	0.6097	0.662	0.7300	0.1203

Figure 15 shows the fractographs for SENT specimens E2-4-1, and E2-4-2 that were obtained after breaking open the SENT specimens using fatigue loads post-test (SENT test specimens were unloaded, after the ductile tearing occurred through part of the initial ligament). A uniform ductile tear crack front obtained at the end of the SENT test in both specimens was observed from the fractographs, since the blunt side-grooves worked effectively. The crack growth of Δa=0.1203 inch in the second test (E2-4-2) was about 1.33 times the Δa=0.0904 inch in the first test (E2-4-1).

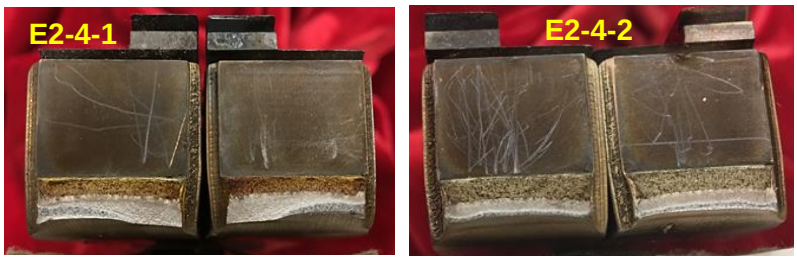

Figure 15. Fracture surface photographs of SENT specimens E2-4-1, and E2-4-2.

Figure 16 shows the load versus load-line displacement curves and load versus COD (clip-gage 1 was close to the surface of the specimen) curves used in the calculation of the fracture toughness parameter, J. The duplicate SENT tests showed very similar results.

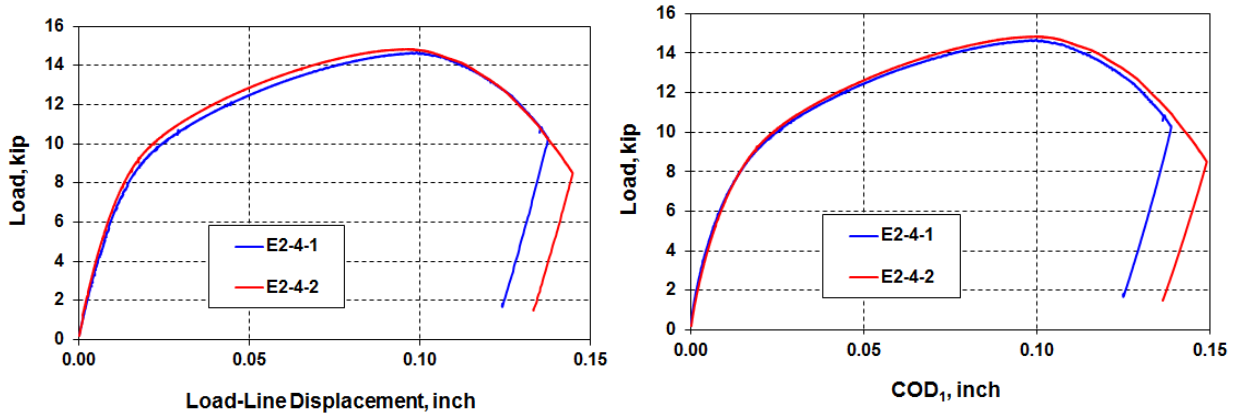

Figure 16. Load versus the load-line displacement and load versus COD_1 from the two SENT tests.

Figure 17 shows the variation of the d-c EP with the COD_1 for the two SENT specimens. Since there is no ASTM test procedure for SENT testing [Kalyanam *et al.*,Wilkowski *et al.*,Hioe *et al.*], the crack initiation and crack growth were both determined by the d-c EP method using Emc^2 SENT test and analysis procedures.

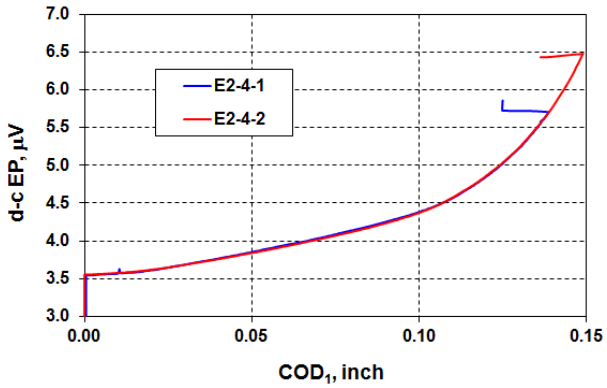

Figure 17. d-c EP variation with COD_1 from the two SENT tests.

Figure 18 shows the variation of the d-c EP with COD_1 along with the region used to select the crack-tip blunting (obtained by fitting a linear-regression line to the variation of d-c EP with COD_1) that occurs prior to crack initiation, as outlined in the earlier work [Wilkowski and Maxey]. The fracture parameters, CTOD and J-value were calculated for the SENT Test E2-4-1 using the measured load, COD, and the d-c EP data and after determination of the crack initiation and crack growth regions. The CTOD could not be determined for SENT specimen E2-4-2, since the clip-gage2 (father from the crack-tip) did not record COD accurately. Hence, the J-value was determined using the clip-gage 1 data (COD1). Since the COD_1 (inner clip-gage) is data measured very close to the SENT crack mouth surface, it closely represents the CMOD, and Figure 20 shows the J-R curve obtained from the two tests using the (inner clip-gage) COD_1 data to represent the CMOD, and the CTOD-R curve obtained from SENT test E2-4-1. The DNV recommended practice [DNV-RP-F108] was originally developed to determine the J-value at crack initiation and the current work used the formulation for obtaining the J-R curves. For a deep crack such as in these SENT tests, the error in calculation of the J_i-values was found to be less than 2%.

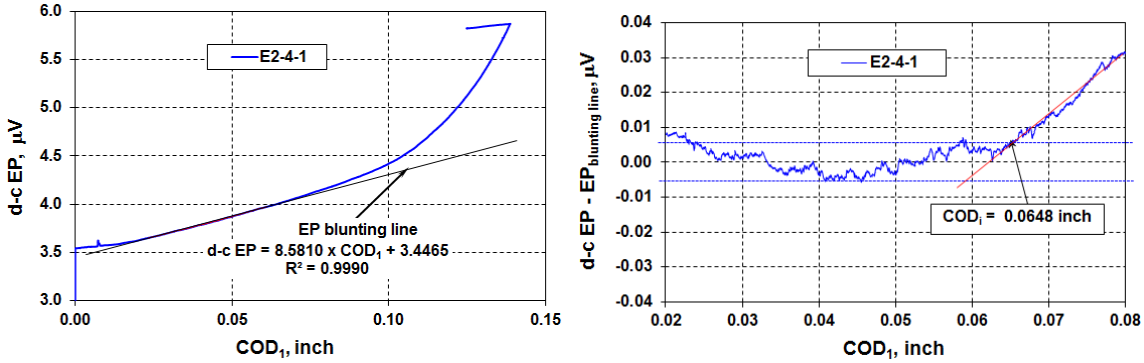

Figure 18. Greatly magnified d-c EP signal versus COD_1 for SENT Specimen E2-4-1, which shows the d-c EP blunting line and the selection of COD_i corresponding to crack initiation.

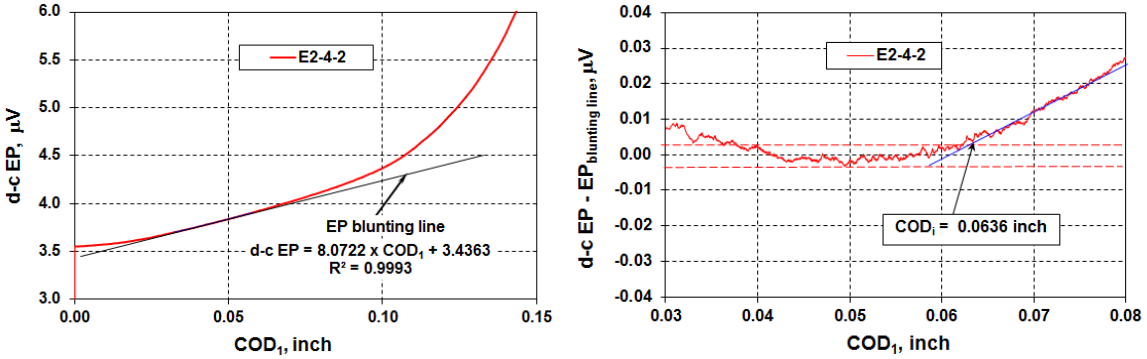

Figure 19. Magnified d-c EP signal versus COD_1 for SENT Specimen E2-4-2, which shows the d-c EP blunting line and the selection of COD_i corresponding to crack initiation.

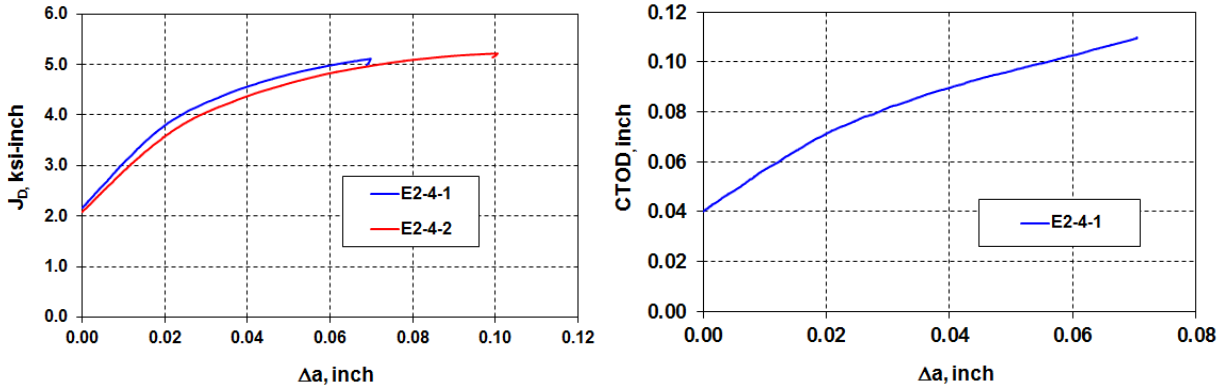

Figure 20. J-R curves obtained from the two SENT specimens, and CTOD-R curve from SENT specimen E2-4-1.

Table 7: Fracture toughness parameters, J, CTOD, and CMOD at crack initiation

Specimen Number	J_i, inch	$CTOD_i$, inch	$CMOD_i$, inch	COD_1, inch
E2-4-1	2.1629	0.0402	0.0610	0.0648
E2-4-2	2.0810	NA*	NA*	0.0636

*NA – Not Available

Figure 21 shows the $J_{initiation}$ value from the elbow experiment FEA (J_i = 2.796 ksi-inch), which was higher than the duplicate SENT tests (average J_i = 2.122 ksi-inch). The IPIRG-2 DRB C(T) specimens gave much higher J_i of 6.206 ksi-inch [Fleming *et al.*]. From this investigation, the elbow had higher fracture toughness than the SENT specimens, but the difference was not as large as observed when comparing the J-values from the TP304 OD SC and the corresponding SENT tests [Hioe, Kalyanam *et al.*]. The difference could perhaps be attributed to the crack driving force differences between the straight-pipe and elbow with SC, and is an area of ongoing research at Emc[2].

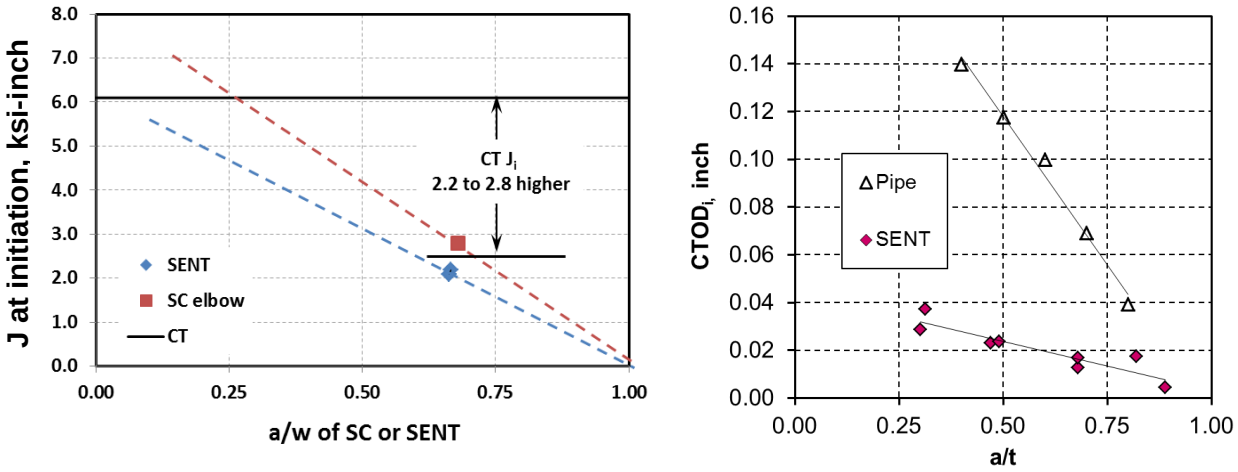

Figure 21. Comparison of $CTOD_i$ values from circumferential surface-cracked straight-pipe and SENT specimens with comparable a/t (a/W) values.

NOMENCLATURE

a/t	Crack depth to thickness ratio
a/W	Crack length to specimen width ratio
ASTM	American Society for Testing and Materials
C(T)	Compact tension (specimen)
CMOD	Crack-mouth-opening displacement
$CTOD_i$	Crack-opening displacement at initiation
CTOD-R	Crack-tip-opening displacement resistance (curve)
d-c EP	direct-current electric potential
EDM	Electric discharge machine
FE	Finite Element
ID	Inner Diameter
IPIRG-2	Second International Pipe Integrity Research Group (program)
J	J-integral fracture parameter
OD	Outer Diameter
SC	Surface Crack
SENT	Single-Edge Notch Tension (specimen)
TWC	Through-Wall Crack

DISCUSSION AND CONCLUSIONS

Findings from investigations on the role of constraint in a circumferentially surface-cracked elbow tested in the IPIRG-2 elbow Experiment 2-4, and SENT specimens with the flaw depth that is same as the deepest point in the ID SC elbow Experiment 2-4 are presented. Using a detailed and precise 3D FEA model of the IPIRG-2 Elbow 2-4 experiment that captured the variable crack depth, variable thickness, and initial ovalization in the elbow, the locations of the largest crack driving force (on Side B of the 180-degree, 70% deep ID SC), J_i at crack initiation loads were determined to select the initial crack depth of $a_o/W=0.68$ for the duplicate SENT specimens tested in this investigation. The following conclusions are drawn, which provide guidance on future investigations that are required when using the fracture toughness (J and CTOD values at specific events like crack initiation) or material fracture resistance curves (J-R) in the prediction of behaviour of surface-cracked pipes and elbows.

- It is normally assumed that the C(T) specimen crack initiation toughness provides a conservative estimate of the material toughness, but it was found in this investigation that the C(T) test $J_{initiation}$ (reported in IPIRG-2 elbow Experiment 2-4 DRB [Fleming *et al.*]) was much higher at 6.206 ksi-inch, when compared to the value of Ji=2.796 ksi-inch for the ID SC elbow 2-4. Since the C(T) specimen crack initiation toughness was about 3 times higher than the ID SC elbow, a check on US NRC PIFRAC database revealed that average Ji value for TP304 C(T) specimens at 550 F was about 7.1 ksi-inch and hence confirming that the IPIRG-2 elbow Experiment 2-4 C(T) J_i=6.206 ksi-inch are a normal test value[2].
- Similarly, the J-value for initiation ($J_{initiation}$) and CTOD at crack initiation (at the start of physical ductile tearing, which is actually a slightly lower J-value than J_{Ic} by ASTM offset definition) when compared between SENT specimen ($a_o/W=0.68$) and elbow with ID SC at the deepest point being (a/t=0.68) revealed that there are some constraint differences which led to the crack initiation toughness of Ji=2.122 ksi-inch in the SENT tests, while it was Ji=2.796 ksi-inch in the ID SC elbow test.
- Comparison of the three geometries, elbow component with ID SC, and specimens CT and SENT revealed very large differences in constraint between the SENT, ID SC elbow and the CT specimens. Although, it is common knowledge that the constraint in the C(T) specimen make the Ji values obtained from this specimen geometry closely represent a TWC in a pipe, this difference between C(T) specimen and the ID SC elbow is new insight to the international technical community.
- This investigation has shown that it is essential to conduct a more in depth study (using experiments and computations) with SENT, C(T), and ID SC elbow geometries with various initial normalized crack depths so as to be able to correlate and use the crack growth resistance curves (J-R, and CTOD-R) fram a SENT or C(T) specimen to a structural integrity assessment of a pipe or elbow component, and pipe system component.
- The material toughness determined at crack initiation, J_i showed that a 68% deep (a/t in ID SC elbow component, and a/W in SENT specimen) was about a factor of three lower than the material crack initiation toughness, J_i determined for a CT specimen (a/W=0.5). This was found to be a significant difference when applied to flaw evaluation methods.
- The constraint effects in the SENT, CT, and the ID SC elbow were analyzed using the J and CTOD values obtained from experiments (material fracture toughness). Alternately, these specimen and component geometries could also be analyzed for the T-stress, J-Q parameters near the crack-tip to understand the crack driving force for fracture in these specimens [Wilkowski, Kalyanam, *et al.*].

[2] Note J_i values in the range of 6.1 ksi-inch are high and hence are not valid plane-strain J_{Ic} values as per ASTM E-1820. The ligament in the specimen is fully plastic. Because it is not a contained plasticity condition, the design of the fracture specimen tests are typically desired to be as close to the full thickness of the pipe as possible to account for geometry effects. Pragmatically, this is a good condition since if it were to be a material with a valid ASTM J_{Ic} value it would break too easily. (Generally such "valid" test results indicate the material is not desirable for service.)

REFERENCES

ASTM E1820, Standard Test Method for Measurement of Fracture Toughness, 2008.

DET NORSKE VERITAS, Recommended Practice DNV-RP-F108 – Fracture Control For Pipeline Installation Methods Introducing Cyclic Plastic Strain, January 2006.

G. Wilkowski, S. Kalyanam, Y. Hioe, F.W. Brust, S. Pothana, M. Uddin, F. Orth, Constraint Effects of Surface Crack Depth on Toughness – Experimental and Numerical Assessments, PVP2019-93713, ASME Pressure Vessels & Piping Conf., San Antonio, Texas, July 14-19, 2019.

G. M. Wilkowski, W.A. Maxey, Review and Applications of the Electric Potential Method for Measuring Crack Growth in Specimens, Flawed Pipes, and Pressure Vessels, Fracture Mechanics 14th Symposium, Vol. II Testing and Applications, ASTM STP 791, Los Angeles, 20 June – 2 July, 1981.

G. Wilkowski, D.J. Shim, S. Kalyanam, G. Wall. P. Mincer, D. Rider, F.W. Brust, D.L. Rudland, Using d-c Electric Potential for Crack Initiation/Growth Monitoring During Testing of Weld Metal Fracture Specimens, Pipeline Technology Conference, Oostende, Belgium, 2009.

M. Fleming, T. Kilinski, P. Scott, G. Wilkowski, Data Record Book Entry E-2.2.2.1 ic.2 for IPIRG-2 Experiment 2-4, 1996.

PipeFracCAE©, Emc2 software for FE mesh generation of pipes, welds, elbows, and advanced FE analysis for stress corrosion cracking simulations.

S. Kalyanam , G. Wilkowski, D.J. Shim, F.W. Brust, Y. Hioe, G. Wall, P. Mincer, Why Conduct SEN(T) Tests and Considerations in Conducting/Analyzing SEN(T) Testing, IPC2010-31631, 8th Intl. Pipeline Conf., Sept. 27 – Oct 1, Calgary, Canada, 2010.

Y. Hioe, S. Kalyanam, G. Wilkowski, Comparison of Unloading Compliance and d-c EP Technique During SENT Testing, Intl. J Pressure Vessels Piping, 156, 79-88, August 2017.

Y. Hioe, S. Kalyanam, G. Wilkowski, S. Pothana, J. Martin, Fracture Toughness Variation with Flaw Depth in Various Specimen Geometries and Role of Constraint in Material Fracture Resistance, PVP2017-65441, ASME Pressure Vessels & Piping Conf., Hawaii, July 16-20, 2017.